SEISMIC FRAGILITY ANALYSIS OF AN ASYMMETRICAL REINFORCED CONCRETE BUILDING CONSDIERING SOIL-STRUCTURE INTERACTION EFFECT

Hyun-Kyu Lim[1], Jun Won Kang[2], Ho-Seok Chi[3], and Moon-Soo Kim[4]

[1] *Department of Civil Engineering, Hongik University, Seoul, Republic of Korea, 04066, limkuy11@gmail.com*
[2] *Department of Civil Engineering, Hongik University, Seoul, Republic of Korea, 04066, jwkang@hongik.ac.kr*
[3] *Department of Structural & Site Safety, Korea Institute of Nuclear Safety, Daejeon, Republic of Korea, 34142, hsc@kins.re.kr*
[4] *Department of Structural & Site Safety, Korea Institute of Nuclear Safety, Daejeon, Republic of Korea, 34142, k181kms@kins.re.kr*

This paper presents the methods for evaluating the seismic fragility and the seismic risk of an asymmetrical reinforced concrete structures considering material nonlinearities. First of all, nonlinear seismic responses of the three-dimensional reinforced concrete structure were evaluated with respect to 100 artificial ground motions with various intensities. To reflect the soil-structure interaction for horizontal, vertical, and rocking oscillations, springs and dampers were introduced at the sides and bottom of the finite element model of foundation. Then seismic fragility of the structure was calculated using the seismic response of the structure based on maximum likelihood estimation method. Maximum inter-story drift was used as earthquake damage indicator, and the thresholds for each damage level were established for the damage assessment of the structure. At last, seismic risk of the structure was evaluated using the seismic fragility of the structure and the seismic hazard curve of exemplary nuclear power plant sites. A method for evaluating the seismic margin of structures was also presented based on the concept of high confidence of a low probability of failure. The series of analyses resulted that the seismic risk of the RC structure was less than 1% in the case that the structure was located at the site of low-to-moderate seismicity area.

I. INTRODUCTION

Seismic fragility of critical civil structures such as bridge, dam, and nuclear power plant structure provides useful data on the seismic design, maintenance, and the evaluation of life-cycle cost of the structures. Results of seismic fragility analysis can be directly used for evaluating the exceeding damage probability of structures during earthquakes with various intensities. This study aims primarily at determining the damage probability and the seismic fragility curve of a three-dimensional reinforced concrete (RC) structure using the seismic response of the structure considering soil-structure interaction effect. This study also aims at evaluating the seismic risk of the structure using the results of seismic fragility analysis and the seismic hazard curve of a site where the structure is to be located.

The target structure of this study is a three-story asymmetrical reinforced concrete building representative of typical half part of a nuclear facility building. The structure is a mock-up structure used for the investigation in SMART 2013 (Seismic design and best-estimate Methods Assessment for Reinforced concrete buildings subjected to Torsion and non-linear effects) international benchmark (Ref. 1, 2). The objectives of the benchmark were to evaluate the conventional design methods of RC structures for the seismic loads of various intensities and to compare analysis methods of the structural dynamic response as well as the floor response spectra from various benchmark participants. This study discusses some of the results of benchmark analyses to validate the three-dimensional finite element model of the SMART 2013 RC structure, and presents the methods for evaluating the seismic fragility and the seismic risk of the structure assuming that the structure is located at a particular nuclear power plant site.

To begin with, finite element modelling of the SMART 2013 RC structure and the results of benchmark simulations comprising modal and nonlinear seismic analyses are presented along with the results of 3D shaking table tests for comparison. Seismic fragility of the structure was calculated using the nonlinear seismic responses of the structure against 100 artificial ground motions. To reflect soil-structure interaction effect, springs and dampers were introduced at the sides and bottom of the finite element model of foundation. Maximum inter-story drift was used as the damage indicator for earthquake, and the thresholds of each damage level were established for the damage assessment of the SMART 2013 RC structure. In the end,

seismic risk of the SMART 2013 RC structure was evaluated using the seismic fragility of the structure and the seismic hazard curve of exemplary nuclear power plant sites. A method for evaluating the seismic margin of structures was also presented based on the concept of high confidence of a low probability of failure.

II. MOMDELLING OF THE SMART 2013 RC STRUCTURE

II.A. Constitutive Models

To model the nonlinear stress-strain relationship of concrete, a constitutive model represented by Eqs. (1) and (2) (Ref. 3) was employed:

$$\sigma = \frac{E_c \epsilon}{1 + \left(\frac{\epsilon}{\epsilon_0}\right)^2} \qquad (1)$$

$$\epsilon_0 = \frac{2f_c'}{E_c} \qquad (2)$$

where σ and ϵ denote stress and strain, respectively. E_c denotes the Young's modulus, f_c' the ultimate compressive strength of concrete, and ϵ_0 the strain at the compressive strength f_c'. For steel reinforcing bars, an elastic perfectly plastic constitutive model was introduced to model its nonlinear stress-strain behavior. The key parameters of the constitutive models are listed in TABLE I, the values of which were provided by the SMART 2013 benchmark.

TABLE I. Material Properties of Concrete and Rebar

Structural components	Young's modulus (MPa)	Poisson's ratio	Compressive strength (MPa)	Tensile strength (MPa)	Mass density (kg/m^3)
Concrete	32,000	0.2	30.0	2.4	2,300
Rebar	210,000	0.3	500	500	7,800

The constitutive model of concrete was approximated by a multi-linear stress-strain relationship as shown in Fig. 1(a), given the material properties in TABLE I. It was modulated that concrete has the modulus of 32,000 MPa in the first line segment, which was followed by five line segments with successively decreasing moduli with respect to strain. Concrete was assumed to behave linearly elastic up to Point 1 until the stress reaches $0.3f_c'$. Points 2, 3, and 4 were obtained from Eq. (1), in which ϵ_0 was calculated from Eq. (2). Stress and strain at Point 5 are f_c' and ϵ_0, respectively. Softening behavior of concrete was approximated by nearly perfectly plastic behavior up to Point 6 at the ultimate strain of 0.003. The yield strength of rebar is 500 MPa at the strain of 0.00238 in both tension and compression, as shown in Fig. 1(b).

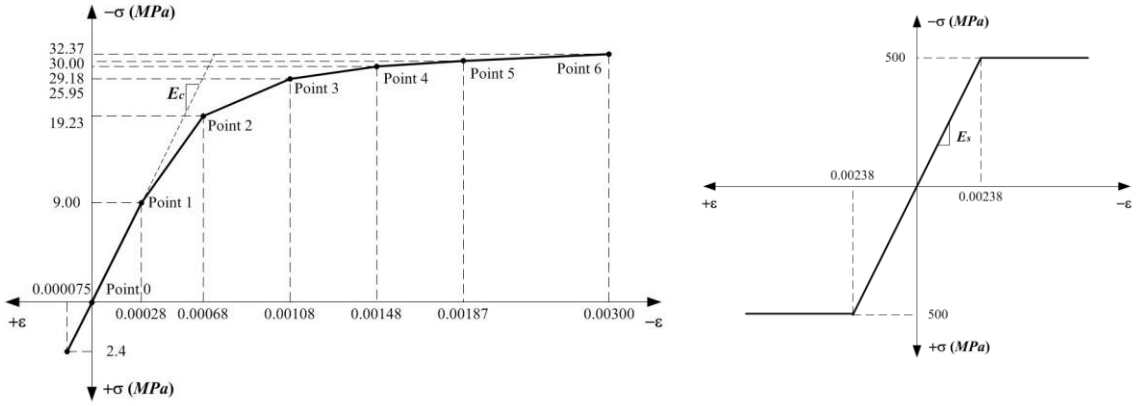

(a) Concrete (b) Steel reinforcement

Fig. 1. Stress-strain relationships of concrete and rebar used for the modelling of SMART 2013 RC structure

II.B. Finite Element Modelling

The SMART 2013 RC structure connected to shaking table was modelled with three-dimensional finite elements, as shown in Fig. 2(a) and 2(b). The model consists of foundation, wall, slab, beam, column, rebar, steel plate, and shaking table. The concrete parts were modelled with an eight-node hexahedral solid element, SOLID65, of ANSYS, whereas the rebar and steel plate were modeled with BEAM188 and SOILD185 elements, respectively. The constitutive relationships of concrete and steel described in Fig. 1 were implemented with the SOLID65 and BEAM188 elements, respectively. Concrete was assumed to show isotropic hardening behavior. Shear transfer coefficient β of the SOLID65 element was set to be 0.5 for open crack and 0.9 for closed crack. To satisfy the compatibility of concrete and steel reinforcement, it was assumed that concrete elements share the node with rebar elements. Fig. 2(c) and 2(d) represents the actuator locations of shaking table and the measurement points of responses, respectively.

(a) SMART 2013 RC structure

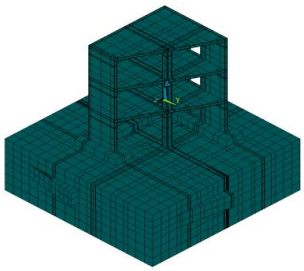

(b) Finite element model of the structure

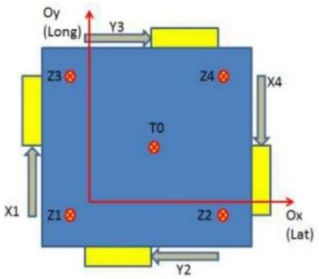

(c) Actuator locations (X1, X4, Y2, Y3, Z1, Z2, Z3, Z4)

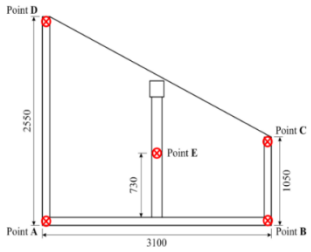

(c) Measurement points

Fig. 2. Modelling of the SMART 2013 RC structure

III. VALIDATION OF THE FINITE ELEMTE MODEL

III.A. Modal Responses

To validate the finite element model of the SMART 2013 RC structure, natural frequencies calculated from modal analysis were compared with the frequencies obtained experimentally. In the modal analysis, structural mass of 11.5 ton, floor mass of 34.4 ton, and the shaking table mass of 25.0 ton were all considered. The actuator locations were set as fixed boundaries. The calculated first three natural frequencies were 6.26Hz, 7.77Hz, and 13.15Hz, respectively, and they were close to experiment results obtained by the SMART 2013 benchmark (Ref. 4) as shown in TABLE II. Modes 1 and 2 represent bending motions of the structure, while mode 3 represents the torsional motion due to the asymmetrical geometry of the structure.

TABLE II. Natural Frequencies Obtained From Modal Analysis and Experiment

	Frequency (Hz)		
	Mode 1	Mode 2	Mode 3
Analysis	6.26	7.77	13.15
Experiment	6.28	7.86	16.50

III.B. Seismic Responses

In addition to the modal analysis, a series of seismic analyses was conducted to validate the finite element model further. Specifically, responses of the structure due to Northridge earthquake ground motion were calculated via nonlinear seismic analysis, and they were compared with experimental responses obtained by shaking table test. Fig. 3(a) shows the time histories of the Northridge earthquake ground motion. The peak ground accelerations (PGAs) are 1.1g and 1.0g in the *x*- and *y*-directions, respectively. The ground motions were applied to the actuator locations at the side and bottom of the shaking table as depicted in Fig. 2(c). Fig. 3(b) exhibits the numerical and experimental responses at sampling point A of the 3rd floor. Overall, the numerical responses agreed well with the experimental results in both amplitude and phase. The absolute maximum displacement and acceleration were 36.73 mm and 22,420 mm/s^2 (2.28g), respectively. Fig. 3(c) depicts the damage due to the shaking table test which occurred in the lower parts of the concrete wall connected to foundation.

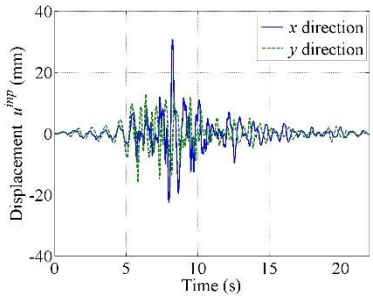

(a) Northridge earthquake

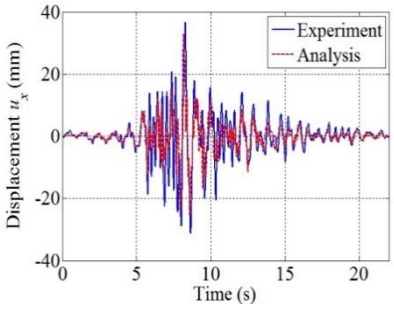

(b) Displacements at point A of the 3rd floor

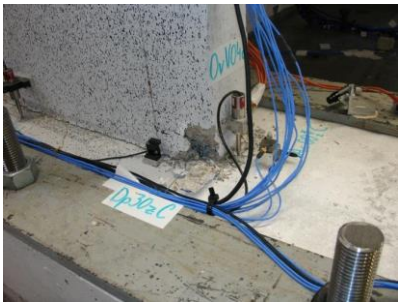

(c) Damage in the concrete wall

Fig. 3 Comparison between the results of nonlinear seismic analysis and shaking table test

IV. SEISMIC FRAGILITY EVALUATION OF THE SMART 2013 RC STRUCTURE

IV.A. Procedure of Seismic Fragility Evaluation

Seismic fragility expresses the conditional probability of failure of a structure for a given seismic motion parameter θ. Given the model response *Y* and the threshold *s* for a damage criterion, the seismic fragility can be represented as the conditional probability that *Y* exceeds the threshold s at the ground motion level of θ:

$$P_f(\theta) = P(Y > s|\theta) \qquad (3)$$

In Eq. (3), the variable *Y* can be generally assumed to be lognormally distributed. Adopting a simple model expressing *Y* as a function of the seismic motion parameter θ, it can be written that $\ln(Y) = a + b\ln(\theta) + \epsilon$, where ϵ is a centered normal Gaussian random variable with standard deviation σ_ϵ. The constants *a* and *b* can be evaluated by means of linear regression. With these notations, the fragility function can be expressed as the cumulative lognormal probability density function as the following:

$$P_f(\theta) = \Phi\left(\frac{\ln(a\,\theta^b/s)}{\sigma_\epsilon}\right) \qquad (4)$$

In nuclear industry, the fragility of a structure is often defined with respect to its capacity, denoted by *A*. The capacity can be defined as the limit seismic load before failure occurs and can be considered as a random variable. If PGA is chosen to characterize seismic load level, then capacity can also be expressed in terms of PGA. The probability of failure, P_f, of a structure under the condition that the structure is subjected to a seismic load with the level of θ can be expressed as:

$$P_f(\theta) = P(failure|\theta) = P(A < \theta) \qquad (5)$$

The capacity is assumed to be lognormally distributed. Then, the seismic fragility, which is the failure probability conditioned on ground motion parameter θ, can be represented by the cumulative density function of capacity *A*:

$$P_f(\theta) = \Phi\left(\frac{\ln(\theta/A_m)}{\beta}\right) \qquad (6)$$

where Φ is the standard Gaussian cumulative density function. With Eq. (6), the fragility curve of a structure can be determined from two parameters: median capacity A_m and lognormal standard deviation β. To evaluate these parameters, a linear regression can be carried out between the sets of $\ln(Y_i)$ and $\ln(\theta_i)$:

$$\ln(Y) = a + b\ln(\theta) \qquad (7)$$

Then, the median capacity A_m can be computed from the coefficients *a* and *b* according to the following expression:

$$\ln(A_m) = \frac{\ln(s) - a}{b} \qquad (8)$$

where s denotes the critical threshold of failure criteria. β stands for the dispersion of the values $\ln(Y_i)$ with respect to the regression curve. It can be computed by the following expression:

$$\beta^2 = \frac{1}{N}\sum_{i=1}^{N}(\ln(Y_i) - \mu_i)^2 \qquad (9)$$

in which $\mu_i = a + b\ln(\theta_i)$.

IV.B. Definition of Damage States

To evaluate the seismic fragility of structures, damage indicator and the thresholds for each damage state should be defined. In this study, maximum inter-story drift at point D of the 3rd floor was used as the quantitative damage indicator, Y. This damage indicator can be useful to investigate the local damage of multi-story structures. Associated with the damage indicator of the maximum inter-story drift, three damage levels were defined: light, controlled, and extended damages. The thresholds for each damage state were defined as the following: $s = h/400$ for light damage, $s = h/200$ for controlled damage, $s = h/100$ for extended damage, where h is the story height of the SMART 2013 structure. Above thresholds for each damage state is based on the recommendation provided by the SMART 2013 international benchmark (Ref. 2).

IV.C. Modelling of Soil-Structure Interaction

In this work, 100 input ground motions with various intensities and frequency contents were used for constructing seismic fragility curves of the SMART 2013 RC structure. The ground motions are synthetic accelerations, generated by a specific generator available in *Code_Aster* (Ref. 2). The accelerations are compatible with median±1σ spectra for a seismic event with magnitude 6.5 in Richter scale and at the distance 9 km from the epicenter. The PGA of the ground motions in the *x*- and *y*-directions ranges from 0.07g to 2.51g and 0.08g to 2.41g, respectively. In calculating the nonlinear seismic response of the SMART 2013 structure, soil-structure interaction effect was considered by modelling springs and dampers between the soil and the foundation with respect to horizontal, vertical, and rocking motions. Fig. 4 shows the schematic view of the SMART 2013 structure with springs and dampers at the foundation. The stiffness and damping coefficients for the modeling of soil-structure interaction effect are presented in TABLE III.

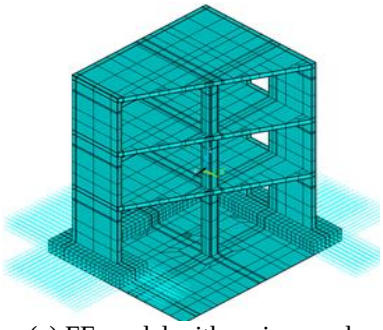

(a) FE model with springs and dashpots at foundation

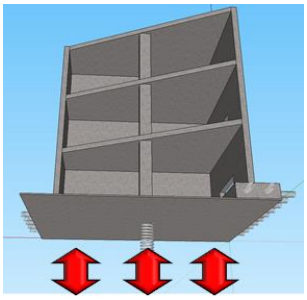

(b) SSI modelling for horizontal and vertical motions

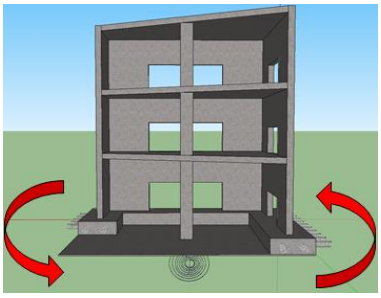

(c) SSI modelling for rocking motion

Fig. 4 Soil-structure interaction modelling of the SMART 2013 RC structure

TABLE III. Parameters for Modelling SSI Effect

Types of motion	Spring stiffness		Damping coefficient	
	Mean value	Coeff. of variation (%)	Mean value	Coeff. of variation (%)
Swaying	3.50×10^8 N/m	1	3.53×10^6 N·s/m	2
Pumping	4.60×10^8 N/m	1	2.63×10^6 N·s/m	2
Rocking in the *x*-direction	6.47×10^8 N·m	1	1.56×10^6 N·s·m	2
Rocking in the *y*-direction	11.30×10^8 N·m	1	3.18×10^6 N·s·m	2

IV.D. Results of Seismic Fragility Analysis

From the nonlinear seismic response of the SMART 2013 RC structure with soil-structure interaction, seismic fragility curves were constructed using the procedure described in Section IV.A. Shown in Fig. 5 are seismic fragility curves of the SMART 2013 structure when the maximum inter-story drift was used as damage indicator. The fragility was calculated with respect to PGA. The fragility analyses showed that the SMART 2013 RC structure was likely to experience light damage for most ground motions, and the probability of exceeding extended damage state was estimated to be over 90% for the ground motion with the PGA level of 1.5 or higher.

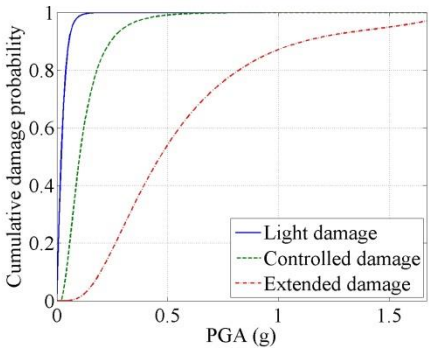

(a) Damage indicator: maximum inter-story drift in the *x*-direction

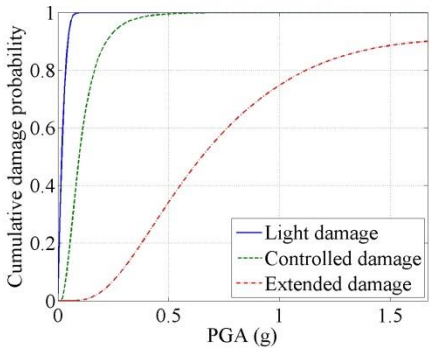

(b) Damage indicator: maximum inter-story drift in the *y*-direction

Fig. 5 Seismic fragility curves of the SMART 2013 RC structure

V. SEISMIC RISK EVALUATION AND SEISMIC MARGIN ASSESSMENT

Probabilistic seismic risk assessment (PSRA) is to determine the probability distribution of the frequency of occurrence of adverse consequences due to earthquakes. In particular, PSRA considers total variability in seismic input, structural response, and structural capacities through engineering models. In this work, seismic risk of structures was defined in terms of the seismic fragility combined with the seismic hazard of a particular site. The seismic risk as well as the seismic margin was evaluated for the SMART 2013 RC structure with the assumption that the structure was located at particular nuclear power plant (NPP) sites.

V.A. Seismic Risk Evaluation

For the seismic risk evaluation of the SMART 2013 RC structure, it is assumed that the structure is located at NPP sites A, B, and C with different levels of seismic hazard. Fig. 6 shows the seismic hazard curves of the three sites illustrating the annual frequency of exceedance of each ground motion level.

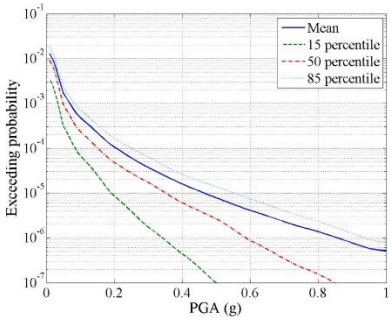

(a) Site A

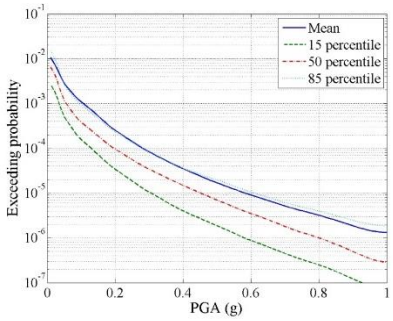

(b) Site B

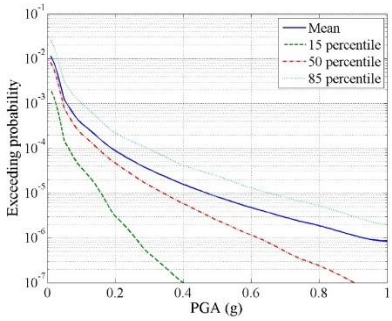

(c) Site C

Fig. 6 Seismic hazard curves of three NPP sites

The seismic risk can be computed from the seismic fragility P_f and the seismic hazard P_H according to the following expression (Refs. 5, 6, 7):

$$P_{sr} = -\int P_f(\theta) dP_H(\theta) \qquad (10)$$

where P_{sr} is the seismic risk and θ denotes the variable representing the intensity of ground motion such as PGA. Using this method, one can take into account the seismic fragility and the annual frequency of exceedance of earthquakes in estimating the seismic risk of a structure. TABLE IV shows the values of seismic risk of the SMART 2013 RC structure calculated at the three NPP sites. The seismic risk was calculated for the damage indicator of maximum inter-story drift in the *x*- and *y*-directions. All values of the seismic risk was less than 1%. The low values of seismic risk are attributed to the fact that the three NPP sites belong to low-to-moderate seismicity area as shown in the seismic hazard curves.

TABLE IV. Results of Seismic Risk Evaluation

NPP sites	Damage indicators	Seismic risk (%)		
		Light damage	Controlled damage	Extended damage
Site A	Maximum inter-story drift in the *x*-direction	0.91	0.66	0.10
	Maximum inter-story drift in the *y*-direction	0.90	0.71	0.12
Site B	Maximum inter-story drift in the *x*-direction	0.79	0.57	0.08
	Maximum inter-story drift in the *y*-direction	0.79	0.61	0.09
Site C	Maximum inter-story drift in the *x*-direction	0.80	0.63	0.15
	Maximum inter-story drift in the *y*-direction	0.80	0.66	0.17

V.B. Seismic Margin Assessment

The seismic risk defined in the previous section is useful in estimating the risk of structural damage with respect to potential earthquakes at a particular site. However, large uncertainties associated with seismic hazard analysis and subjective inputs used in the seismic fragility evaluation could make the result of seismic risk evaluation less reliable. In this study, seismic margin was explored based on the concept of the high confidence of low probability of failure (HCLPF) capacity to complement the seismic risk. The HCLPF capacity can be determined as the PGA corresponding to the 5 percent probability of failure in the seismic fragility curve with 95 percent confidence level. Fig. 7 shows the seismic fragility curves of the SMART 2013 RC structure used for the evaluation of HCLPF capacity. The HCLPF capacity can also be computed by the following equation with the parameters described in Section IV.A (Ref. 5):

$$\text{HCLPF(PGA)} = A_m e^{-1.65\beta} \qquad (11)$$

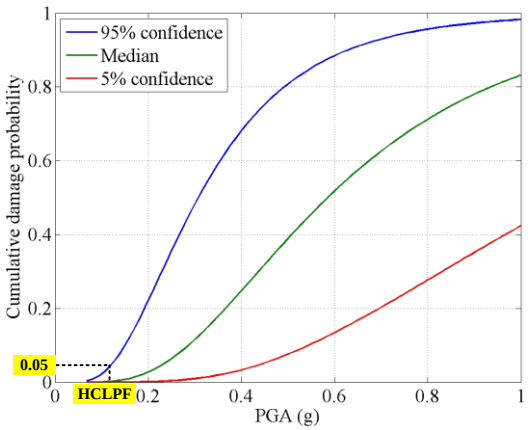

Fig. 7. Determination of HCLPF capacity from seismic fragility curve

TABLE V shows the HCLPF capacities calculated for the SMART 2013 RC structure. The HCLPF capacities were computed using the damage indicator of maximum inter-story drift in the *x*- and *y*-directions. If the safe shutdown earthquake (SSE) of the considered NPP sites is about 0.2-0.3g, it can be concluded that the SMART 2013 RC structure has bare seismic margin with respect to the SSE of the investigated NPP sites.

TABLE V. Results of Seismic Margin Assessment

Damage indicator	HCLPF capacity (PGA)
Maximum inter-story drift in the *x*-direction	0.16 g
Maximum inter-story drift in the *y*-direction	0.22 g

VI. CONCLUSIONS

This paper presented the method of evaluating the seismic fragility of RC structures using the seismic response with soil-structure interaction effect. This paper also discussed the method of evaluating the seismic risk and the seismic margin of structures using the seismic fragility data and the seismic hazard curve of a particular site. The target structure is a three-dimensional asymmetrical reinforced concrete building investigated in the SMART 2013 international benchmark. The fragility analyses showed that the SMART 2013 RC structure was likely to experience light damage for most ground motions, and the probability of exceeding extended damage state was estimated to be over 90% for the ground motion with the PGA level of 1.5 or higher. The seismic risk analysis resulted that the seismic risk of the SMART 2013 RC structure was less than 1% in the case that the structure was located at the site which belonged to low-to-moderate seismicity area. Seismic margin of the structure was evaluated based on the concept of high confidence of a low probability of failure. From the calculated HCLPF capacity, it could be concluded that the SMART 2013 RC structure had bare seismic margin with respect to the SSE of about 0.2-0.3g.

ACKNOWLEDGMENTS

This research was supported by the Korea Institute of Nuclear Safety (grant No. 14-51), and by the Korea Institute of Energy Technology Evaluation and Planning (KETEP) (grant No. 20151520100990). The supports are greatly appreciated.

REFERENCES

1. T. Chaudat, P.E. Charbonnel, C. Garnier, M. Le Corre, M. Mahe, S. Poupin and S. Vasic, “SMART 2013 test report,” NT14-019, French Alternative Energies and Atomic Commission (2014)
2. B. Richard, M. Fontan and J. Mazars, “SMART 2013: overview, synthesis and lessons learnt from the international benchmark,” NT14-037, French Alternative Energies and Atomic Commission (2014)
3. D. Kachlakev and T. Miller, “Finite element modeling of reinforced concrete structures strengthened with FRP laminates-final report,” FHWA-OR-RD-01-17, Oregon Department of Transportation (2001)
4. T. Chaudat and B. Richard, “SMART 2013 data acquisition project,” NT13-003, French Alternative Energies and Atomic Commission (2013)
5. J.W., Reed and R.P. Kennedy, “Methodology for Developing Seismic Fragilities,” EPRI/TR-103959, Electric Power Research Institute (1994)
6. H.M. Koh, J.H. Lee and J.W. Kang, “Seismic Damage Evaluation of Reinforced Concrete Pier Based on a Plastic Damage Model,” *Journal of Korea Society of Civil Engineering*, **23**, 5, pp. 1029-1039 (2003)
7. T.H. Kim, Y.J. Kim, and H.M. Shin, “Seismic performance assessment of reinforced concrete bridge piers supported by laminated rubber bearings,” *Structural engineering and mechanics: An international journal*, **29**, 3, pp. 259-278 (2008)